EPR of Cu^{2+} Prion Protein Constructs at 2 GHz Using the $g_\perp$ Region to Characterize Nitrogen Ligation

James S. Hyde,[†*] Brian Bennett,[†] Eric D. Walter,[‡] Glenn L. Millhauser,[‡] Jason W. Sidabras,[†] and William E. Antholine[†]

[†]Department of Biophysics, Medical College of Wisconsin, Milwaukee, Wisconsin; and [‡]Department of Chemistry and Biochemistry, University of California, Santa Cruz, California

ABSTRACT A double octarepeat prion protein construct, which has two histidines, mixed with copper sulfate in a 3:2 molar ratio provides at most three imidazole ligands to each copper ion to form a square-planar Cu^{2+} complex. This work is concerned with identification of the fourth ligand. A new (to our knowledge) electron paramagnetic resonance method based on analysis of the intense features of the electron paramagnetic resonance spectrum in the $g_\perp$ region at 2 GHz is introduced to distinguish between three and four nitrogen ligands. The methodology was established by studies of a model system consisting of histidine imidazole ligation to Cu^{2+}. In this spectral region at 2 GHz (S-band), *g*-strain and broadening from the possible rhombic character of the Zeeman interaction are small. The most intense line is identified with the $M_I = +1/2$ extra absorption peak. Spectral simulation demonstrated that this peak is insensitive to cupric A_x and A_y hyperfine interaction. The spectral region to the high-field side of this peak is uncluttered and suitable for analysis of nitrogen superhyperfine couplings to determine the number of nitrogens. The spectral region to the low-field side of the intense extra absorption peak in the $g_\perp$ part of the spectrum is sensitive to the rhombic distortion parameters A_x and A_y. Application of the method to the prion protein system indicates that two species are present and that the dominant species contains four nitrogen ligands. A new loop-gap microwave resonator is described that contains ~1 mL of frozen sample.

INTRODUCTION

This work describes an improved electron paramagnetic resonance (EPR) methodology for interpreting spectra from Cu^{2+} square-planar complexes to determine the number of nitrogen ligands. All EPR spectra were obtained at low microwave frequencies—either 2 or 3.3 GHz—with the use of loop-gap resonators (LGR) (1,2). The method was applied to a standard sample, copper histidine, which has four equivalent nitrogen ligands. The study was then extended to a copper-binding domain derived from the prion protein (PrP), where the number of nitrogen ligands is uncertain.

Rist et al. (3) and Rist and Hyde (4) showed that the values of the Zeeman and hyperfine parameters for a square-planar copper complex are strongly affected by the molecular environment, and that rhombic distortion can occur. Furthermore, in powders and glasses containing these complexes, line broadening (termed *g*-strain and *A*-strain) is always encountered. In a molecular orbital formulation, broadening arises from the distributions of bonding parameters. Froncisz and Hyde (5,6) noted that the $g_\parallel$ ''turning points'' in the derivative-like spectra from square-planar copper complexes can be considered identical to pure absorption spectra from single crystals in the parallel orientation, as was previously pointed out for other highly anisotropic systems (7,8). Froncisz and Hyde discovered that distributions of $A_\parallel$ and $g_\parallel$ at these turning points, the so-called *g*- and *A*-strains, were correlated, tending to cancel for $M_I = -1/2$ or $-3/2$ and to add for $+1/2$ and $+3/2$. They introduced the term ε for the correlation coefficient. If this term is greater than zero, the $g_\parallel$ $M_I = -1/2$ feature always exhibits the best resolution. Their calculations indicated that the spectral resolution of superhyperfine couplings to ligand nitrogen nuclei is expected to be optimal at a microwave frequency of 2 GHz, which is near the lower end of the S-band range. At this frequency, the *g*- and *A*-strain distributions cancel to a degree that is determined by ε, and the number of nitrogen ligands can, it was hypothesized, be determined. Froncisz and Aisen (9), in a study of monocupric transferrin, provided the first experimental demonstration of these ideas. This theory was subsequently applied to numerous copper systems (10–12) in studies that addressed copper binding in PrPs. In those studies, the microwave frequency was ~3.3 GHz, which was a compromise between optimal resolution and reasonable signal/noise ratio (SNR).

This methodology was found to be robust in distinguishing between the cases of 0, 1, 2, or 3 nitrogen ligands, but distinguishing between three and four nitrogen ligands has proven difficult. In a simple stick diagram, coupling to three equivalent nitrogen nuclei results in seven superhyperfine lines of relative intensities 1, 3, 6, 7, 6, 3, and 1, whereas for four nitrogen nuclei, the relative intensities of the nine-line pattern are 1, 4, 10, 16, 19, 16, 10, 4, and 1. It is noted that the nitrogen hyperfine coupling is nearly isotropic (4), and stick-diagram analysis is therefore appropriate. The SNRs have been inadequate for reliable detection of the

Submitted November 3, 2008, and accepted for publication January 26, 2009.

*Correspondence: jshyde@mcw.edu

Editor: David D. Thomas.

0006-3495/09/04/3354/9 $2.00

doi: 10.1016/j.bpj.2009.01.034

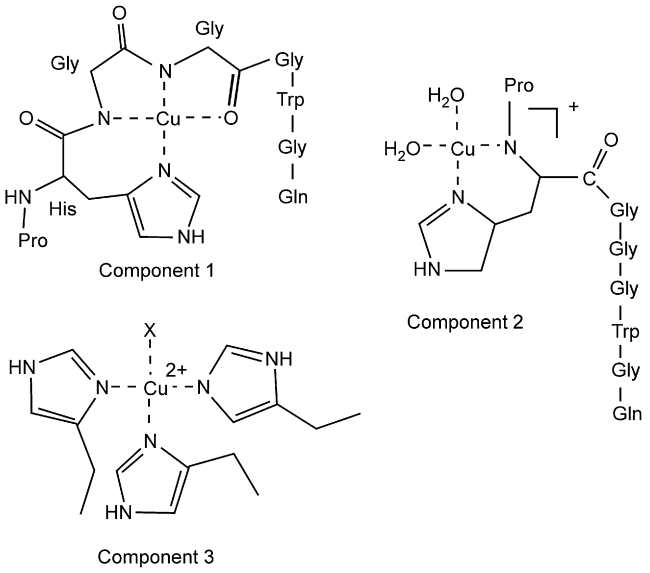

FIGURE 1 Copper complexes of the prion octarepeat peptide system.

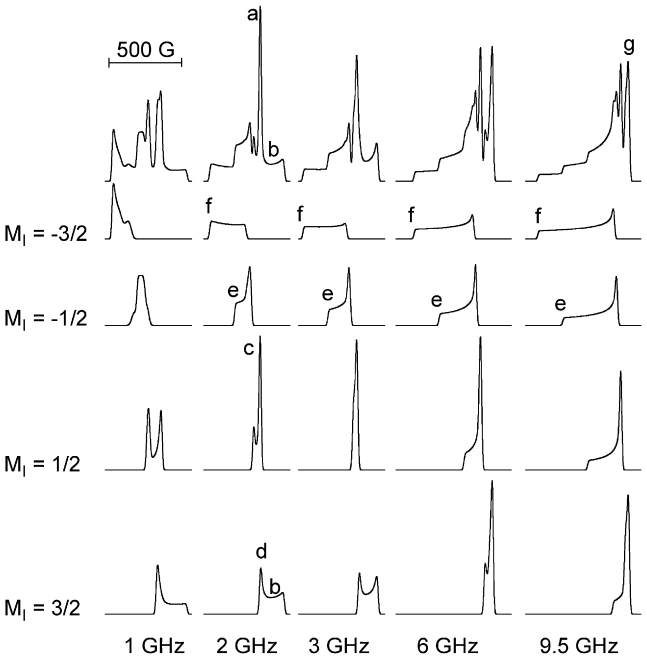

FIGURE 2 Simulated pure absorption square-planar Cu^{2+} spectra as a function of frequency together with simulations of the four copper hyperfine manifolds that form the spectra (see text for details).

weakest lines, and the relative intensities of the three most intense lines are nearly the same (6/7 compared with 16/19) for three and four nitrogen nuclei, respectively. Hyde et al. (13) pointed out that the ratios of signal intensities of the second and third lines from the center to the intensity of the center line can be diagnostic in determining whether three or four nitrogens are present.

The PrP binds Cu^{2+} in its N-terminal octarepeat domain, comprised of tandem PHGGGWGQ octarepeat segments. Recent work from our laboratories demonstrates the existence of three distinct copper-binding modes depending on the precise ratio of Cu^{2+} to octarepeat concentrations (12). At high occupancy, each HGGGW segment, within an individual octapeptide, takes up a single Cu^{2+} equivalent. Equatorial coordination involves the histidine imidazole and deprotonated amide nitrogens from the two glycines that immediately follow the histidine. At low copper occupancy, coordination is from imidazole nitrogens involving three or four histidine side chains. These two binding modes, referred to as component 1 and component 3, respectively (see Fig. 1), are well characterized. Component 2 coordination is observed at intermediate copper concentrations; however, the precise details of this binding mode are less certain. EPR investigations using selectively *N*-methylated peptides suggest that there are two nitrogens at equatorial coordination sites: one from the histidine imidazole, and one from the histidine backbone nitrogen. However, the 3.3 GHz EPR spectra derived from these constructs were not well resolved and thus were ambiguous regarding the exact number of equatorial nitrogens. In addition, the prion fragment with two octarepeats has not been studied in detail. In this study, we applied 2 GHz EPR to Cu^{2+}-PrP constructs with the goal of obtaining greater resolution and detail with regard to the equatorial coordination environment. This was a joint project conducted by the prion-construct team at the University of California, Santa Cruz, and the microwave resonator team at the Medical College of Wisconsin. At the outset of the project, the sample volume was set at 1 mL. Sample preparation and development of a purpose-built 2 GHz LGR suitable for a 1 mL sample were carried out at the same time.

It was expected that the increase in sample volume from 70 μL to 1 mL would more than compensate for the loss of sensitivity at 2 GHz relative to 3.3 GHz, and that improved resolution of the $g_{\|}$ $M_I = -1/2$ feature would permit determination of the number of nitrogen ligands (three or four) for the particular prion construct of interest. As it turned out, this expectation failed.

However, during the course of the research, what we consider a new, successful way to determine the number of nitrogen ligands for square-planar Cu^{2+} complexes was found based on analysis of the $g_{\perp}$ part of the spectrum. This new method is the primary subject of the study presented here. The idea is illustrated in Fig. 2. The top row shows ideal simulated pure absorption Cu^{2+} spectra at 1, 2, 3, 6, and 9.5 GHz, and the lower rows show the spectral manifolds assigned to the four copper nuclear quantum numbers. The integrated areas of spectra in the first row are identical, and the integrated areas of spectral manifolds assigned to each of the four copper nuclear transitions are each 1/4 of the integrated area of spectra in the first row. All spectra were simulated using the same linewidth, all ligands were assumed to have zero nuclear spin, and only one copper isotope was assumed to be present. Axial

TABLE 1 Characteristics of 3.3 and 2 GHz resonators

Parameters	3.3 GHz one-loop/one-gap	2 GHz one-loop/one-gap
Inner radius, R	2.29 mm	5.5 mm
Outer radius, r	4.83 mm	7.5 mm
Gap width, w	2.54 mm	2.0 mm
Gap separation, t	0.217 mm	0.424 mm
Resonator height, Z	10.16 mm	12.70 mm
Sample tube I.D.	3 mm	9 mm
Sample wall thickness	0.5 mm	0.5 mm
Frequency calculated	3.360 GHz	2.071 GHz
Frequency measured	3.309 GHz	1.962 GHz
Q_0-value calculated	1825	2658
Q_0-value measured	1717	1664
Efficiency, Λ	4.94	2.09
Sample volume	0.0718 mL	0.8079 mL
Resonator volume	0.1674 mL	1.2069 mL
Filling factor, η	0.4150	0.6209
Shield inner diameter	20.32 mm	21.59 mm

symmetry was assumed, with the principal axes of the Zeeman and Cu-hyperfine interactions colinear. The radio-frequency (RF) magnetic field was assumed to be strictly perpendicular to the applied field. Spectral features of interest in the following discussion are lettered in Fig. 2 for convenience.

Intense features are seen in the so-called $g_\perp$ region of the spectra. These features have variously been called ''overshoot'' lines, extra absorption (EA) peaks, or hyperfine anomaly lines in the literature. They are associated with $M_I = +1/2$ and $+3/2$ spectral manifolds. The earliest explanation of these features seems to be that of Ovchinnikov and Konstaninov (14), who introduced the EA notation. As is apparent, these features arise from a buildup of intensity arising from the interplay of g- and A-anisotropies. At 6 and 9.5 GHz, two EA transitions are seen, whereas at 2 and 3 GHz, there is just one. In this study, we focus on the feature (labeled a) seen at 2 GHz. To the high-field side of a, there is a broad, featureless region of nearly zero intensity in a derivative-like display (labeled b). Region b is favorable for the observation of superhyperfine coupling to nitrogen nuclei.

Variation of these couplings occurs if the nitrogen ligands are inequivalent, which affects resolution. Using electron-nuclear double resonance (ENDOR), Rist and Hyde (4) found that the nitrogen nuclear superhyperfine tensor exhibits a small degree of rhombicity, which can be expected to be unresolved in EPR but will contribute to broadening of superhyperfine coupling.

Cancellation of the g- and A-strains occurs to varying degrees in the parallel features e and f arising from $M_I = -1/2$ and $-3/2$ transitions. For all other transitions (parallel as well as perpendicular), the g- and A-strains add. $A_\perp$ is much smaller than $A_\parallel$, and the spectral features associated with $A_\perp$ will, we expect, exhibit correspondingly reduced strain broadening. At sufficiently low microwave frequencies, the g-strain no longer dominates the residual linewidth. Thus, as an alternative to analyzing features e and f to count nitrogens, we propose a strategy for analysis in the more intense perpendicular part of the spectrum. We seek a sufficiently low microwave frequency to avoid dominant g-strain broadening and to identify a spectral feature with minimal overlap that is dominated only by residual $A_\perp$ strain. Our working hypothesis is that feature a and the high-field side of this feature, region b, satisfy these requirements at 2 GHz. Peak a is a superposition of peaks c and d, although peak c is strongly dominant. At this frequency, we expect to see, without overlap, the intense center superhyperfine line and either three or four transitions to the high-field side with intensities that match (by computer fitting) the assignment to either three or four nitrogen ligands.

In the course of developing the methodology introduced in this work, we considered the possibility that some amount of rhombicity could be present, requiring that $g_\perp$ and $A_\perp$ be divided into components g_x, g_y, A_x, and A_y, respectively. Of course, as the microwave frequency is reduced, Zeeman rhombic distortion becomes increasingly difficult to detect. We carried out simulations similar to those of Fig. 2, using the parameters given by Rist et al. (3). At a microwave frequency of 2 GHz, the low-field side of the EA transition (Fig. 2 a) was found to be sensitive to hyperfine rhombicity, whereas the high-field side was insensitive.

MATERIALS AND METHODS

Resonator design and construction

LGR design was carried out with the use of Ansoft (Pittsburg, PA) High Frequency Structure Simulator (HFSS, version 10.1) software, which provides full-wave solutions to Maxwell's equations and also can find resonant frequencies using an eigenmode solver. Ansoft Maxwell 3D (version 11), which is based on a quasi-static approximation to Maxwell's equations, was used to determine eddy currents arising from magnetic field modulation. Simulations were performed with a sample that had the dielectric constant of ice ($\varepsilon_r = 3.2 + j0.00128$) (15) in the appropriate quartz tube ($\varepsilon_r = 3.78$) (see Table 1 for sample tube and resonator dimensions). Values are also provided for the resonator used to acquire spectra at 3.3 GHz (see Fig. 3). Both LGRs were of the one-loop/one-gap type (1) (see Fig. 3).

The dimensions of the resonator were adjusted until the resonator frequency with the sample in place was 2 GHz. Modulation slots were then added to the design, and simulation of field modulation penetration was carried out using Ansoft Maxwell 3D.

An assembly drawing using three-dimensional computer-aided design was prepared using AutoDesk (San Rafael, CA) Inventor 10, and fabrication drawings of each part were made using the symbolic language of geometric dimensioning and tolerancing. Most parts were made using wire electrical discharge machining. In this technique, both the LGR gap and field modulation slots can be as small as 0.05 mm, with precisional tolerances of 0.001 mm. The resonator body was made from high-purity silver (see Fig. 4). Table 1 gives measured and calculated parameters comparing the resonator of Fig. 4 with the structure that has been used in this laboratory for more than 20 years (2).

Relative sensitivities were determined from simulations of electromagnetic fields under both the assumption of constant incident power and the assumption of constant peak value of H_1 (the RF magnetic field in the rotating frame) at the sample. The latter condition is equivalent to assuming that T_1 (the electron spin-lattice relaxation time) is independent of

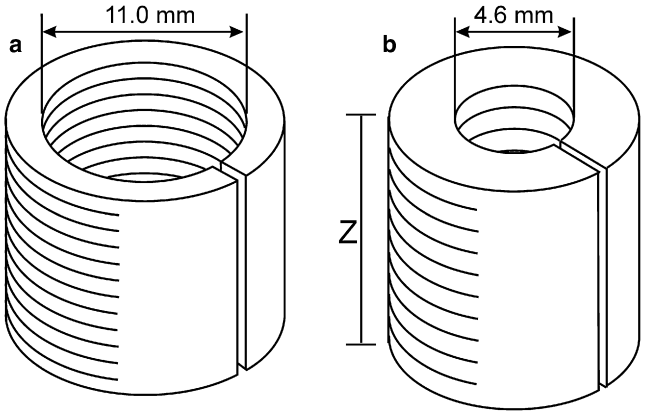

FIGURE 3 LGR outline drawings: (*a*) 2 GHz; (*b*) 3.3 GHz. (See Table 1 for additional dimensions.)

microwave frequency and that spectra are acquired in all cases at the same degree of microwave power saturation.

Relative sensitivities at the same level of incident power can be calculated using the data in Table 1 and the theory outlined by Feher (16); the subscripts refer to resonators *a* and *b* of Fig. 3:

$$\frac{S_a}{S_b} = \frac{\omega_a}{\omega_b}\frac{\eta_a}{\eta_b}\frac{Q_a}{Q_b} = 0.88.$$

The filling factors in Table 1 were calculated using HFSS. Under this condition, the loss in sensitivity because of the linear dependence of the Boltzmann factor on microwave frequency is compensated for by the increase in filling factor, and the resultant sensitivity is nearly the same at 3.3 and 2 GHz. This increase arises because a lower fraction of the 2 GHz resonator is occupied by sample-cell walls.

Relative sensitivities at the same level of microwave field can be calculated using the theory as outlined by Hyde and Froncisz (2). Here, the sample volume is V and the RF field is assumed to be uniform over the sample:

$$\frac{S_a}{S_b} = \frac{\omega_a}{\omega_b}\frac{\Lambda_a}{\Lambda_b}\frac{V_a}{V_b} = 2.85.$$

The increase in sensitivity at 2 GHz under the condition of constant RF field at the sample arises from increased sample volume. From a practical perspective, the spectra reported here have about the same SNR at 2 and 3.3 GHz.

Simulation

EPR spectra were calculated with the XSophe suite of programs (17), employing matrix diagonalization and a mosaic misorientation linewidth model-based algorithm (17,18). Matrix diagonalization was required because the condition of applicability of perturbation theory for the simulation of Cu^{2+} ceases to hold at frequencies below ~2 GHz (14). Correlated strains in g and A (5,6) were included, largely to account for the lineshapes of the $g_{\|}$ features of the Cu^{2+} spectra (19). The linewidth is expressed, in frequency terms (20,21), by the formula

$$\sigma_\nu^2 = \left(\sum_{i=x,y,z}\left\{\sigma_{\mathrm{Ri}}^2 + \left[(\sigma g_i/g_i)\nu_0(B)+\sigma A_i M_i\right]^2\right\}g_i^2 I_i^2\right)/g^2,$$

where

$$\sigma_{\mathrm{Ri}}(i = x,y,x)$$

are the residual linewidths due to unresolved hyperfine coupling and other sources, and σg_i and σA_i are the widths of Gaussian distributions of g_i and A_i, respectively.

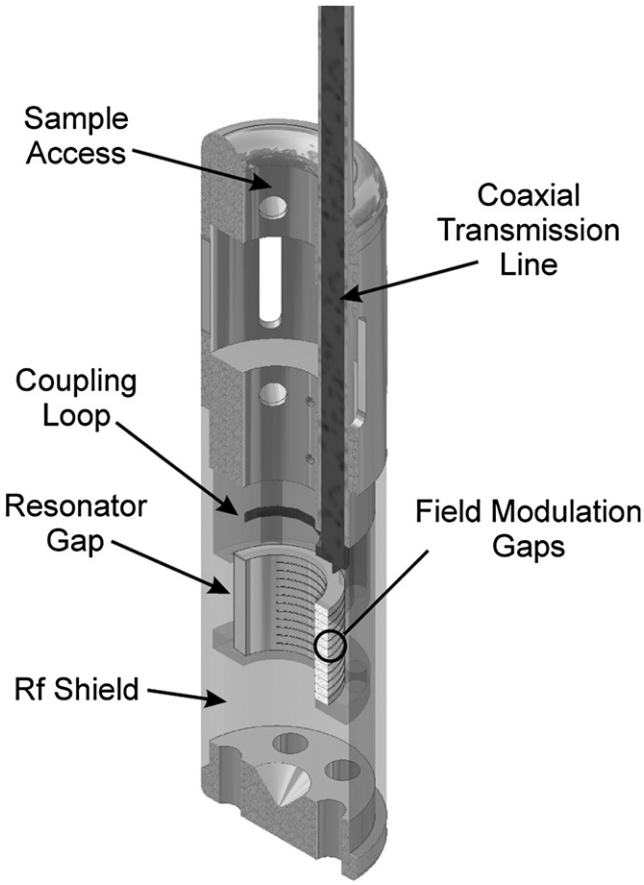

FIGURE 4 Cutaway drawing of the 2 GHz LGR assembly. The sample passes through the coupling loop. For adjustment of the coupling, the resonator (with sample) moves and the coupling loop is fixed. The shield is fiberglass-epoxy-plated on the inside. Temperature-regulated gas flows over the assembly for temperature control.

Simulations were carried out over field ranges of 600–1000 G using 4096 points and sampling 240 partitions, and four segments of the Sophe grid (17) (see Table 2 for simulation parameters).

Sample preparation

A copper histidine sample, which is known to have four equivalent in-plane nitrogen ligands, was prepared to test the use of the $g_\perp$ spectral region to determine the number of nitrogens. The sample was prepared by adding ^{63}Cu (2 mM final concentration; Cambridge Isotope Laboratories, Andover, MA) to excess (40 mM) histidine (enzyme grade; Fisher BioReagents, Fairlawn, NJ) in 20% glycerol.

The PrP construct consists of amino acids 23–27 followed by 60–75 (22). It was prepared using fluorenylmethoxycarbonyl (Fmoc) methods as described previously (12). The sequence was KKRPKPHGGGWGQPHGGGWGQ. This section of the sequence is common to all placental mammals except mice. The construct concentration was 600 μM in D_2O/NEM buffer (25 mM ethylmorpholine) at pH 6.5 (pD = 6.1) with 20% glycerol. The copper concentration was 400 μM of ^{63}Cu (copper sulfate). Thin-walled (0.5 mm) quartz sample tubes with inner dimensions of 3 mm for 3.3 GHz experiments and 9 mm for 2 GHz experiments were used.

EPR spectroscopy

The S-band spectrometer consists of a Varian E-9 EPR spectrometer fitted with a microwave bridge of local design and construction operating between

TABLE 2 Simulation parameters

CuIm at 1.896 GHz
$g_{i\ (i = x,\ y,\ z)} = 2.056, 2.056, 2.261$ $\lvert A_i(^{63}\text{Cu})\rvert = 2.0, 2.9, 18.5 \times 10^{-3}\ \text{cm}^{-1}$ $\lvert A_i(^{14}\text{N})\rvert = 1.43, 1.43, 1.27 \times 10^{-3}\ \text{cm}^{-1}$ Linewidth, $\sigma_{Ri} = 0.50, 0.50, 0.25 \times 10^{-3}\ \text{cm}^{-1}$ g-strain, $\sigma g_i/g_i = 0.0007, 0.0007, 0.0005$ A-strain, $\sigma A_i/A_i = -0.5, -0.5, -0.8 \times 10^{-3}\ \text{cm}^{-1}$
Model simulations (1–9.5 GHz)
$g_i = 2.079, 2.079, 2.298$ $\lvert A_i(^{63}\text{Cu})\rvert = 2.4, 2.4, 18.5 \times 10^{-3}\ \text{cm}^{-1}$ Linewidth, $\sigma_{Ri} = 0.8, 0.8, 0.8 \times 10^{-3}\ \text{cm}^{-1}$
Prion parameters (1.949 GHz)
$g_i = 2.061, 2.061, 2.248$ $\lvert A_i(^{63}\text{Cu})\rvert = 2.8, 2.8, 17.2 \times 10^{-3}\ \text{cm}^{-1}$ $\lvert A_i(^{14}\text{N})\rvert = 1.34, 1.34, 1.20 \times 10^{-3}\ \text{cm}^{-1}$ Linewidth, $\sigma_{Ri} = 0.70, 0.70, 0.30 \times 10^{-3}\ \text{cm}^{-1}$ g-strain, $\sigma g_i/g_i = 0.0030, 0.0030, 0.0005$ A-strain, $\sigma A_i/A_i = 0.5, 0.5, -1.0 \times 10^{-3}\ \text{cm}^{-1}$

1.98 and 4 GHz. A Varian flow system was used to control the temperature. The EPR facilities are located at the National Biomedical EPR Center at the Medical College of Wisconsin (Milwaukee, WI), sponsored by the National Institutes of Health.

The spectrometer conditions for 2 GHz spectra for copper histidine were as follows: microwave frequency, 1.8922 GHz; microwave power, 2.8 mW; modulation frequency, 100 kHz; time constant, 0.128 s; modulation amplitude, 3 G; scan time, 4 min; four scans averaged for 1000 G scans; and −140°C.

The spectrometer conditions for 2 GHz spectra for the cupric complex of PrP(23–27, 60–75), Cu-KKRPK(PHGGGWGQ)2, were as follows: microwave frequency, 1.925 GHz; microwave power, 10.5 mW; modulation frequency, 100 kHz; time constant, 0.128 s; modulation amplitude, 7 G; scan time, 4 min; five scans averaged across 1000 G scans; and −140°C.

Corresponding values at 3.3 GHz were the same except for the following: microwave power, 2.2 mW; modulation amplitude, 7 G; scan time, 1 min; and 18 scans averaged across 1000 G.

RESULTS

Copper histidine

The EPR spectrum of Cu^{2+}-histidine (Cu-His) exhibits a resolved superhyperfine pattern at the $M_I = -1/2$ $g_\parallel$ line, centered at around 510 G (Fig. 5 *a*; the $M_I = -3/2$ line is not shown). Seven lines would be expected for three nitrogen ligands of Cu^{2+}, and nine lines for four nitrogens; the SNR of the experimental spectrum is too poor to distinguish these possibilities by direct observation. The pattern at $g_\parallel$ ($M_I = -1/2$) contains a center line (labeled "0") and therefore comprises an odd number of lines. Intense, well-resolved lines, due primarily to the $M_I = +1/2$ and $-1/2$ manifolds (see Fig. 2), were also observed in the $g_\perp$ region from ~620 to 740 G.

Computer simulations of the experimental spectrum are presented as traces *b–e* of Fig. 5, for which the number of nitrogen ligands and the hyperfine interaction with ^{63}Cu in the *x-y* plane were varied. Positions of superhyperfine nitrogen transitions for the $M_I = -1/2$ $g_\parallel$ feature, and also for the high-field side of the EA line, which is feature *a* in Fig. 2, are indicated in Fig. 5. Fig. 6 shows, in expanded form, the fits that have been obtained for the superhyperfine spectra of Cu-His for three and four nitrogen ligands. Fig. 6 *a* is for the $M_I = -1/2$ line in the parallel region of the spectrum, and Fig. 6 *b* is a fit to the superhyperfine pattern on the high-field side of the perpendicular region of the spectrum. Even with the aid of computer simulation, determination of the number of nitrogens using the $g_\parallel$ region alone is not convincing. However, the outermost line on the high-field side in the $g_\perp$ region (*line 4* of Fig. 6 *b*) is observed in both the experimental spectrum and in the simulation with four equivalent nitrogen ligands, but not in the simulation with three. In addition, the ratio of the heights of line 2 to line 0 in the $g_\perp$ region is diagnostic. This ratio is sensitive to the assignment of ligation to either three or four nitrogens, and the fit is much better for four than for three.

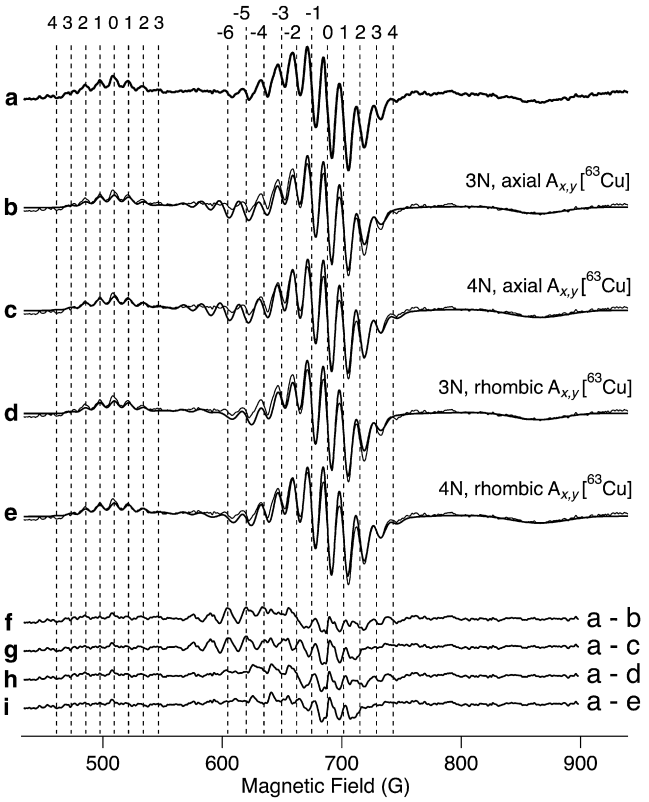

FIGURE 5 (*a*) EPR spectrum of Cu-His at 2 GHz. (*b*) Simulation for three nitrogen ligands and axial $A(^{63}\text{Cu})$ ($A_\perp = 2.4 \times 10^{-3}\ \text{cm}^{-1}$). (*c*) Simulation for four nitrogen ligands and axial $A(^{63}\text{Cu})$ ($A_\perp = 2.4 \times 10^{-3}\ \text{cm}^{-1}$). (*d*) Simulation for three nitrogen ligands and rhombic $A(^{63}\text{Cu})$ ($A_x = 2.0 \times 10^{-3}\ \text{cm}^{-1}$, $A_y = 2.9 \times 10^{-3}\ \text{cm}^{-1}$). (*e*) Simulation for four nitrogen ligands and rhombic $A(^{63}\text{Cu})$ ($A_x = 2.0 \times 10^{-3}\ \text{cm}^{-1}$, $A_y = 2.9 \times 10^{-3}\ \text{cm}^{-1}$). (*f–i*) Residuals. In traces *b–e*, the computed spectra (*bold lines*) are overlaid on the experimental spectra (*thin lines*). Labeled, dashed lines show the superhyperfine transitions used to determine the number of ligands (lines 0–4) and to aid refinement of the A_x and A_y ^{63}Cu hyperfine terms (lines −3 to −6). Note the much improved fit in the range of 550–620 G when the rhombicity of the copper hyperfine tensor is included.

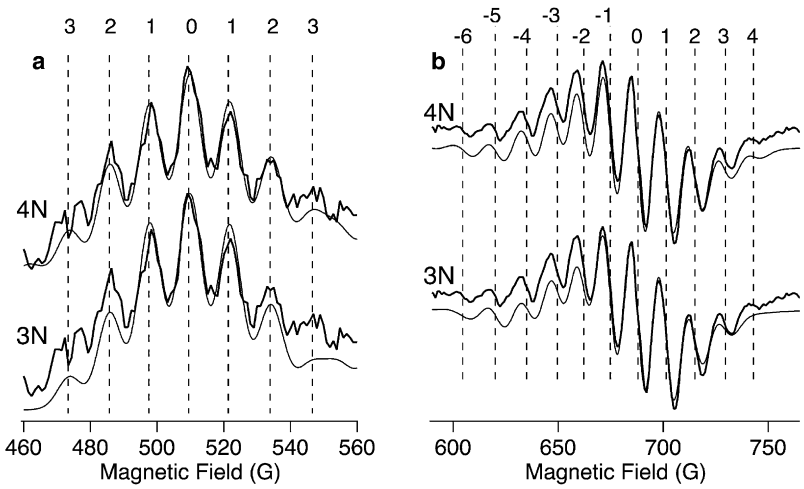

FIGURE 6 Superposition of calculated spectra (*thin lines*) on the experimental spectra (*thick lines*) of Cu-His in spectral regions used to determine the number of nitrogen ligands. (*a*) The $g_{\|}$ $M_I = -1/2$ region of the spectrum. (*b*) the $g_{\perp}$ region of the spectrum. Simulations assumed either three (labeled "3N") or four ("4N") nitrogen ligands with the same parameters as for Fig. 5, *d* and *e*, respectively. The labeled, dashed lines signify superhyperfine transition lines in the spectra, as in Fig. 5.

In this nearly ideal system, the SNR in the parallel region remains insufficient to distinguish between three and four nitrogens, although this might be possible using more extensive signal averaging. The known assignment to four nitrogens is clearly supported in the perpendicular region of the spectrum by the analysis presented here. The experimental evidence for line 4 and the substantially improved fits to the intensities of lines 2 and 3 are judged to be definitive. Residuals *g* and *i* in Fig. 5, which are for four nitrogens, are substantially reduced in the range of 720–750 G relative to *f* and *h*, which are for three nitrogens. This example supports the hypothesis that spectral fitting of the $g_{\perp}$ region at 2 GHz can be used to determine the number of nitrogen ligands.

Although the fit of the nitrogen superhyperfine features on the high-field side of the $M_I = 1/2$ EA line seen in Fig. 5 *c* for four equivalent nitrogens is very good, the fit of spectral features on the low-field side of the EA line fails. In particular, see lines labeled -5 and -6. The only remaining free parameter within the assumptions of the model is $A_{\perp}$. Spectral features on the low-field side of the EA line were found to be quite sensitive to this parameter, but the fits still remained unsatisfactory under the assumption of an axial copper hyperfine tensor. Therefore, the decision was made to add a small amount of rhombicity to the model. Parameters A_x and A_y were swept, and a convincing fit of lines labeled -3 to -6 was achieved (Figs. 5 *e* and 6 *b*). (See residuals *h* and *i* compared with *f* and *g* in Fig. 5.) The spectra were insensitive to rhombic distortion of the Zeeman tensor, presumably because of the low magnetic field required for 2 GHz EPR.

The lines on the low-field side of the $M_I = +1/2$ EA line arise from a superposition of the superhyperfine pattern that is centered on the EA line onto patterns from other hyperfine manifolds (see Fig. 2). The perpendicular feature of the $M_I = -1/2$ manifold is prominent among the features of these other manifolds. The resultant overlap of nitrogen superhyperfine lines from different copper hyperfine manifolds is very sensitive to the copper hyperfine values. The existence of overlapping superhyperfine lines makes the 2 GHz spectrum sensitive to hyperfine coupling. The molecular structure that gives rise to the observed rhombicity is unknown, but is thought to arise from steric effects of the bulky ligand groups.

Thus, we propose that in a sample of unknown nitrogen ligation, the most intense line in the $g_{\perp}$ region of the spectrum should first be located and the number of well-resolved lines to the high-field side in this pattern should then be counted. If the center line is designated as "0", four more lines are resolved in the case of four nearly equivalent nitrogen donor atoms in the equatorial plane. Using this analysis, the number of nitrogen donor atoms is determined from the intense lines in the perpendicular spectral region arising from the $+1/2$ EA manifold. After this step, the analysis can be extended, if desired, to the copper hyperfine couplings in the perpendicular orientation.

Cu^{2+} plus excess KKRPK(PHGGGWGQ)$_2$

The increase in spectral resolution of the $-1/2$ $g_{\|}$ feature of the PrP construct at 1.925 GHz compared with 3.275 GHz, due to greater cancellation of the strain terms, is readily evident (Fig. 7). However, the SNR is not sufficient to distinguish a nine-line pattern from a seven-line pattern. The resolution of the superhyperfine couplings in the $-1/2$ $g_{\|}$ feature is also poorer (comparing Fig. 7 with Figs. 5 and 6), which may arise because one of the four nitrogen ligands is not equivalent to the other three ligating nitrogens.

The $g_{\|}$ $M_I = +3/2$ and $-3/2$ features in Fig. 7 are nonsymmetric, unlike the corresponding features from the imidazole model system (Figs. 5 and 6). This is spectroscopic evidence for the presence of at least two species with differing coordination. These species could also lead to loss of superhyperfine resolution.

In the $g_{\perp}$ region, the resolution is improved at 1.925 GHz relative to 3.275 GHz (Fig. 7) but is poorer relative to

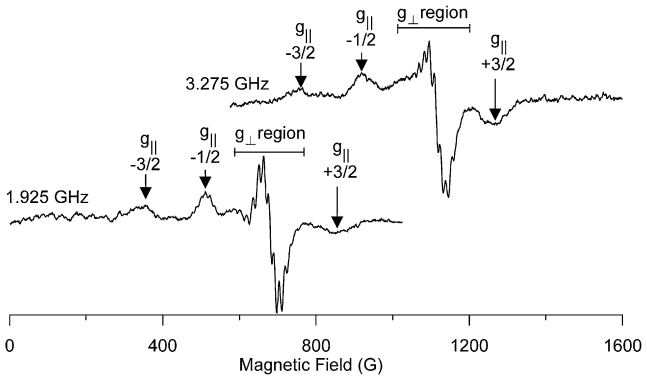

FIGURE 7 Copper spectra of the double octarepeat prion peptide at 3.275 and 1.925 GHz (see text for details).

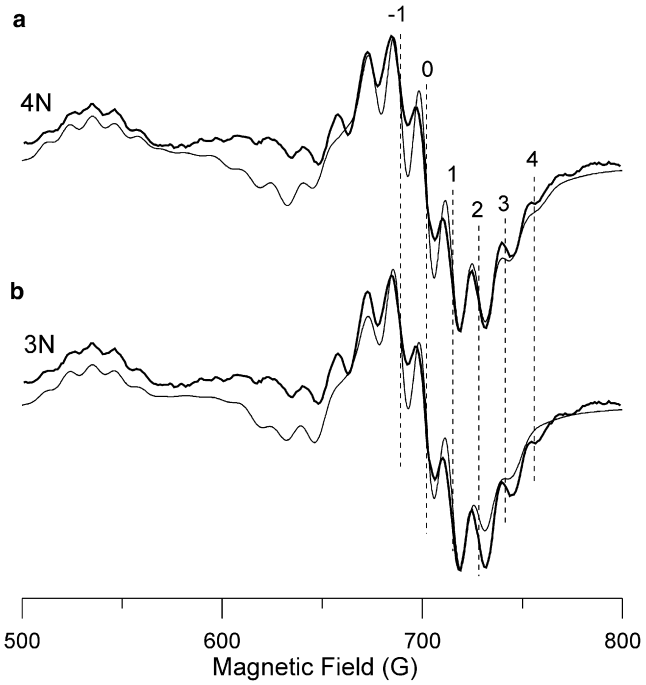

FIGURE 8 (*a*) Simulations for four equivalent nitrogen ligands superimposed on the experimental 1.925 GHz spectrum of Fig. 7. (*b*) Spectral fit for three equivalent nitrogens.

copper-histidine spectra (Figs. 5 and 6). The methodology developed for interpretation of the superhyperfine structure in the perpendicular region of the spectrum of the imidazole model system was applied to the PrP construct using an increased intrinsic linewidth. The most intense line corresponds in position to the EA transition and is assigned to line 0 of the nitrogen superhyperfine spectrum, and spectra are simulated for three and four nitrogen ligands. The results are shown in Fig. 8, *a* and *b*, where the fit was forced by setting both peak-to-peak intensities to the same value. The fit of transitions labeled 2, 3, and 4 is substantially better for 4N compared to 3N. These are transitions that are particularly sensitive to the number of nitrogen ligands (13). The spectral positions for lines 0 and ± 1 are good, but the intensities of these lines are in poor agreement. It is possible that spectral contributions from spurious species with 0, 1, or 2 nitrogen ligands underlie the spectrum. A change of ligation can be expected to shift an EA line, resulting in linewidth increase of lines 0 and 1 of the superimposed superhyperfine patterns. Because of these uncertainties, no attempt was made to fit the features to the low-field side of the EA peak.

It is concluded that the dominant species present in the PrP preparation has four nitrogen ligands, and that both $g_{\|}$ and $g_{\perp}$ portions of the spectrum are consistent with the presence of more than one species.

DISCUSSION

Based on the studies presented here on the copper histidine system in frozen solution, it is concluded that EPR at 2 GHz solves resolution problems associated with *g*-strain broadening in the so-called perpendicular region of the spectrum. It can be speculated that unresolved coupling to nearby protons, the anisotropy of the nitrogen nuclear hyperfine couplings, nonequivalent nitrogen ligands, and the precise choice of microwave frequency will determine the linewidth.

We have demonstrated that features to the high-field side of the most intense spectral feature of copper imidazole at 2 GHz—namely, the EA line—can be well simulated by the assumption of isotropic coupling to four nitrogen ligands.

Many spectral simulations were performed in the course of this work, and the existence of an easily recognized, well-defined EA peak associated with the $+1/2$ copper nuclear hyperfine manifold was robust. The $+3/2$ $g_{\|}$ turning point is to the high-field side of the EA line, but it is weak and diffuse. All studies performed to date support the hypothesis that the spectral region to the high-field side of the EA line can be used to distinguish between four-nitrogen ligation and three-nitrogen/one-oxygen ligation.

Features to the low-field side of the EA line, including rhombicity, are sensitive to $A_{\perp}$. The value of $A_{\perp}$ has not, to the best of our knowledge, previously been determined by analysis of EPR powder-type spectra. It was hypothesized that a scan of the $A_{\perp}$ value to achieve a best fit of the features to the low-field side of the most intense spectral feature would permit determination of this difficult-to-measure parameter. The results support the hypothesis that EPR at 2 GHz permits determination of the A_x and A_y components of $A_{\perp}$.

Of the four spectral features assigned to the so-called parallel region of the spectrum, the $M_{\mathrm{I}} = -1/2$ feature exhibits the highest superhyperfine resolution. Improved resolution arises from a canceling of *g*-strain by correlated *A*-strain. Acquisition at 2 GHz is favorable, and longer acquisition times than were used here are recommended. Nevertheless, the method described herein will generally be favored because of the 10-fold higher signal intensities of the $M_{\mathrm{I}} = +1/2$ EA line in the perpendicular part of the spectrum relative to the $M_{\mathrm{I}} = -1/2$ feature in the parallel part of

the spectrum. It can be presumed that strains in the parallel and perpendicular regions will differ since they arise fundamentally from distributions of different combinations of bonding parameters. Little is known about strain in the perpendicular spectral region.

The 2 GHz LGR described here was specifically designed for this experiment. The sample volume of ~1 mL was preset by the constraints of preparing the PrP construct. Modeling of the resonant microwave frequency with the sample was within 2% of the value observed. The coupling structure was also computer-modeled, taking into account the calculated Q-value with the sample, and worked as expected. The choice of microwave frequency was based on the analysis of Froncisz and Hyde (5). This is the frequency that is predicted to yield the narrowest superhyperfine linewidth for the $M_I = -1/2$ $g_{||}$ feature. Accidentally, this choice proved to be favorable for the analysis method introduced here. Fig. 2 suggests that 3 GHz would be more favorable than 2 GHz, but Fig. 7 indicates for the protein construct that spectral resolution in the perpendicular part of the spectrum is substantially poorer at 3.275 GHz relative to 1.925 GHz. The optimum microwave frequency for our method appears to be ~2.5 GHz. It is noted that LGRs that contain 1 mL of sample can readily be designed throughout the 2–4 GHz band.

The spectroscopic EPR evidence presented here shows that the dominant component present in the double octarepeat PrP construct can be simulated using four equivalent equatorial nitrogen ligands. In region *b* of the spectrum as defined in Fig. 2, the relative intensities of lines 2, 3, and 4 are nearly the same for both the PrP construct and the Cu-His sample that was studied in this work (compare Fig. 6 *b* with Fig. 8 *b*). This assignment is consistent with the results of Chattopadhyay et al. (12). Component 3 was observed in the presence of excess octarepeat and assigned to a species with three equatorial histidines plus either an unknown oxygen or a nearly equivalent additional in-plane nitrogen ligand. Component 1 was considered by Burns et al. (10). It was formed using a stoichiometry of about one octarepeat to one copper and contains just one histidine nitrogen. Additional nitrogen ligands are nonequivalent. The resolution of copper superhyperfine structure in the $-1/2$ $g_{||}$ feature is much poorer for component 1 than for component 3 (12), which is consistent with the nonequivalence of the nitrogen ligands in component 1. For the PrP system studied here, three histidines are available for every copper ion. The spectroscopic data presented here support the presence of a heterogeneous sample, with one component consisting of four nearly equivalent nitrogen ligands (possibly all from histidines) and the other component or components consisting of complexes with either one or two nitrogens. If the two-nitrogen component is present, nonequivalence would be expected to result in further broadening of lines 0 and 1, as was observed. A spectrum similar to that found for component 2 was reported for the full PrP (11). It is possible that this component can be assigned to one of the superimposed spectra in this study.

At 2 GHz, the EPR spectra of Cu^{2+} square-planar copper spectra exhibit increased resolution in the $g_{\perp}$ spectral region for several reasons: 1), g-strain is greatly reduced and no longer dominant over other line-broadening mechanisms; 2), rhombicity of the Zeeman interaction is not apparent; and 3), only one EA line occurs, as demonstrated in Fig. 2. We show here for the copper-histidine system that this spectral region can be reliably simulated. These simulations permit determination of the rhombicity of the copper hyperfine coupling and of the number of equatorial nitrogen ligands, which up to now has been an elusive goal. Moreover, it may be within reach to determine whether all nitrogen ligands are equivalent. It may even be possible to determine the anisotropy of the superhyperfine couplings, as suggested by the residual, line *i* of Fig. 5. Experiments as a function of increasing microwave frequency can be expected to yield quantitative information about g-strain in the perpendicular spectral region, as well as Zeeman rhombicity. Experiments involving decreasing frequency, including experiments with the microwave field H_1 parallel to H_0, will provide information about the copper quadrupole coupling, as shown previously (23). Global fitting of multifrequency spectra can be expected to yield magnetic parameters with increased precision. LGRs are the enabling technology for low-frequency EPR, and further development of this technology is possible.

This work was supported by National Institutes of Health grants R01 EB001417 and P41 EB001980 (J.S.H.), and R01 GM065790 (G.L.M).

REFERENCES

1. Froncisz, W., and J. S. Hyde. 1982. The loop-gap resonator: a new microwave lumped circuit ESR sample structure. *J. Magn. Reson.* 47:515–521.
2. Hyde, J. S., and W. Froncisz. 1989. Loop gap resonators. *In* Advanced EPR: Applications in Biology and Biochemistry. A. J. Hoff, editor. Elsevier, Amsterdam, The Netherlands. 277–306.
3. Rist, G. H., J. Ammeter, and H. H. Günthard. 1968. Influence of the host lattice upon the EPR coupling parameters of copper-8-hydroxyquinolinate. *J. Chem. Phys.* 49:2210–2217.
4. Rist, G. H., and J. S. Hyde. 1969. Ligand ENDOR of Cu-8-hydroxyquinolinate substituted into organic single crystals. *J. Chem. Phys.* 50:4532–4542.
5. Froncisz, W., and J. S. Hyde. 1980. Broadening by strains of lines in the g-parallel region of Cu^{2+} EPR spectra. *J. Chem. Phys.* 73:3123–3131.
6. Hyde, J. S., and W. Froncisz. 1982. The role of microwave frequency in EPR spectroscopy of copper complexes. *Annu. Rev. Biophys. Bioeng.* 11:391–417.
7. Hubbell, W. L., and H. M. McConnell. 1971. Molecular motion in spin-labeled phospholipids and membranes. *J. Am. Chem. Soc.* 93:314–326.
8. Weil, J. A., and H. G. Hecht. 1963. On the powder line shape of EPR spectra. *J. Chem. Phys.* 38:281–286.
9. Froncisz, W., and P. Aisen. 1982. The EPR spectra of copper transferrin complexes at 2–4 GHz. *Biochim. Biophys. Acta.* 700:55–58.
10. Burns, C. S., E. Aronoff-Spencer, C. M. Dunham, P. Lario, N. I. Avdievich, et al. 2002. Molecular features of the copper binding

sites in the octarepeat domain of the prion protein. *Biochemistry*. 41:3991–4001.

11. Burns, C. S., E. Aronoff-Spencer, G. Legname, S. B. Prusiner, W. E. Antholine, et al. 2003. Copper coordination in the full-length, recombinant prion protein. *Biochemistry*. 42:6794–6803.
12. Chattopadhyay, M., E. D. Walter, D. J. Newell, P. J. Jackson, E. Aronoff-Spencer, et al. 2005. The octarepeat domain of the prion protein binds Cu(II) with three distinct coordination modes at pH 7.4. *J. Am. Chem. Soc*. 127:12647–12656.
13. Hyde, J. S., W. E. Antholine, W. Froncisz, and R. Basosi. 1986. EPR determination of the number of nitrogens coordinated to Cu in square-planar complexes. *In* Advanced Magnetic Resonance Techniques in Systems of High Molecular Complexity, Vol. 2. N. Niccolai and G. Valensin, editors. Birkhäuser, Boston. 363–384.
14. Ovchinnikov, I. V., and V. N. Konstaninov. 1978. Extra absorption peaks in EPR spectra of systems with anisotropic *g*-tensor and hyperfine structure in powders and glasses. *J. Magn. Reson.* 32:179–190.
15. Westphal, W. B., and A. Sils. 1972. Dielectric Constant and Loss Data. Laboratory for Insulation Research, Massachusetts Institute of Technology, Cambridge, MA.
16. Feher, G. 1957. Sensitivity considerations in microwave paramagnetic resonance absorption techniques. *Bell System Tech. J*. 36:449–484.
17. Hanson, G. R., K. E. Gates, C. J. Noble, A. Mitchell, S. Benson, et al. 2003. XSophe-Sophe-XeprView: a computer simulation software suite for the analysis of continuous wave EPR spectra. *In* EPR of Free Radicals in Solids: Trends in Methods and Applications. M. Shiotani and A. Lund, editors. Kluwer Press, Amsterdam, The Netherlands. 197–237.
18. Shaltiel, D., and W. Low. 1961. Anisotropic broadening of line-width in the paramagnetic resonance spectra of magnetically dilute crystals. *Phys. Rev*. 124:1062–1067.
19. Basosi, R., W. E. Antholine, and J. S. Hyde. 1993. Multifrequency ESR of copper: biophysical applications. *In* Biological Magnetic Resonance. Vol. 13. L. J. Berliner and J. Reuben, editors. Plenum, New York. 103–150.
20. Pilbrow, J. R. 1990. Transition Ion Electron Paramagnetic Resonance. Clarendon, Oxford.
21. Pilbrow, J. R., G. R. Sinclair, D. R. Hutton, and G. J. Troup. 1983. Asymmetric lines in field-swept EPR: Cr^{3+} looping transitions in ruby. *J. Magn. Reson.* 52:386–399.
22. Stahl, N., and S. B. Prusiner. 1991. Prions and prion proteins. *FASEB J*. 5:2799–2807.
23. Liczwek, D. L., R. L. Belford, J. R. Pilbrow, and J. S. Hyde. 1983. Elevation of copper nuclear quadrupole coupling in thiol complexes by completion of the coordination sphere. *J. Phys. Chem.* 87:2509–2512.